**Proceedings Paper:**

Kiring, A., Salman, N., Liu, C. et al. (2 more authors) (2016) A. Kiring, C. Liu, N. Salman, I. Esnaola, L. Mihaylova, A Shrinkage-based Particle Filter for Tracking with Correlated Measurements. In: Sensor Data Fusion: Trends, Solutions, Applications (SDF), 2015. Sensor Data Fusion: Trends, Solutions, Applications (SDF), 2015, 06-08 Oct 2015, Bonn, Germany. IEEE .

https://doi.org/10.1109/SDF.2015.7347704

# A Shrinkage-based Particle Filter for Tracking with Correlated Measurements

Aroland Kiring, Naveed Salman, Chao Liu, Iñaki Esnaola, Lyudmila Mihaylova

Department of Automatic Control and Systems Engineering
University of Sheffield, United Kingdom
{*amkiring1, n.salman, cliu47, esnaola, l.s.mihaylova*}*@sheffield.ac.uk*

***Abstract*—This paper studies the problem of tracking with wireless sensor networks (WSNs) using received signal strength (RSS) measurements. The log-normal shadowing associated with RSS measurements from a mobile terminal is correlated both in space and time. We propose a particle filter that exploits the temporal and spatial correlation and estimates the covariance matrix of the measurement noise using the shrinkage technique. Simulation results show that using the estimated covariance matrix in the tracking filter improves considerably the filter performance. It is also demonstrated via simulations that the shrinkage-based particle filter exhibits superior performance to the particle filter without shrinkage when limited measurements are available. Results with high accuracy of tracking using the proposed method are presented.**

## I. Introduction

A wireless sensor network (WSN) usually consists of hundreds or thousands of multi-functional sensors, which are randomly deployed in a surveillance area. These sensor nodes are able to sense and communicate wirelessly to exchange information. Wireless sensor technologies are widely used in many applications, e.g., in health-care, earth sensing, defence and agriculture. Tracking in WSNs is based on different types of measurements, such as the angle of arrival (AOA) [1], time of arrival (TOA) [2], time difference of arrival (TDOA) [3] and the received signal strength (RSS) [4], [5]. Both the AOA and TOA provide better accuracy in distance estimation than the RSS. However, the AOA technique relies on the presence of a multi-antenna array, while the TOA technique requires highly synchronized clocks between the transmitter and the receiver. Therefore, these techniques require additional hardware to be implemented. The RSS techniques have less accuracy, but offer simplicity and low cost of implementation.

The Kalman filter (KF) is a widely used estimator method that provides an optimal solution when the system is linear. However, if the system is non-linear, the KF faces challenges. Alternative KF variants are the extended Kalman filter (EKF) [6], [7] and the unscented Kalman filter (UKF) [8]. The EKF operates by linearizing the non-linear system model and measurement model, and the UKF improves on this by providing an estimate with higher-order accuracy [9]. However, when the non-linearities in the system model or in the measurement model become too severe, these filters produce unreliable estimates. Most of the non-linear KF and their variants assume that the system states follow a Gaussian distribution but in practical applications, this assumption is often invalid. Remarkably, the particle filter (PF) can be applied to non-linear systems with non-Gaussian signals. PF operates by estimating the time varying state of a dynamic system that cannot be observed directly and is observed through alternative related measurements instead. The tracking accuracy of PF is influenced by several design parameters in the algorithm, such as the number of generating particles, measurement noise and sampling frequency. When large number of particles is used, the tracking accuracy of the PF improves. However, this comes at a heavy computational cost.

Most PF tracking algorithms and measurement methods assume that the measurement noise is additive and has a constant covariance matrix describing the second order moments. Unfortunately, this assumption is only applicable if the target is static. However, when the target is moving, the distance between each sensor and the target varies greatly. Consequently, the measurement noise covariance also varies with time. Furthermore, most of the RSS-based location estimation methods assume that, individual channels between the target and sensor nodes are independent of each other. This is not valid as readings from the mobile target at the sensor nodes introduce an element of spatial-temporal correlation. In this study, the correlated measurements are simulated using the Gudmundson correlation model [10].

Covariance is a measure of the relationship between two variables and plays an important role in many applications. In finances, the covariance matrix of stock indexes is used to estimate the stock returns [11] and in bioinformatics, the covariance matrix of genes is used to perform gene classifications [12]. A simple method to estimate the covariance matrix is to use a sample estimator. The sample estimator can give an accurate estimation of the covariance matrix if a large number of observations is available. However, in many applications, only small and limited number of observations are available. That being the case, the shrinkage method is introduced. In this paper, the shrinkage method is used to estimate the covariance between readings of different sensor nodes from a single target to enhance the performance of the PF algorithm.

The rest of the paper is organized as follows. Section II describes the tracking system model for single target tracking. Section III, reviews the shrinkage method. Section IV, presents the details of the proposed shrinkage-based PF for dealing with correlated measurements. Section V evaluates the performance of the proposed shrinkage-based PF. Finally, section VI presents the conclusion.

## II. TRACKING SYSTEM MODEL

A single mobile node in a two-dimensional (2-D) plane with coordinates $(x, y)$ is considered. Sensors are uniformly deployed in the field of interest with known locations $(x_i, y_i)$ for $i = 1, 2, \ldots, n_s$, where $n_s$ is the number of sensor nodes. These coordinates can be obtained using a global positioning system (GPS), or by installing sensors at points with known coordinates. The following notations are defined; $(\cdot)^T$ is the transpose operator, $E[\cdot]$ is the expectation operation, and $\mathbf{I}$ denotes the identity matrix.

### A. Target Mobility Model

Various mobility models have been developed over time such as random walk mobility models, pursue mobility models, and Singer-type mobility models [13], [14]. The discrete-time Singer-type mobility model [15] is adopted because it represents strongly correlated accelerations and allows the prediction of the position, speed, and acceleration of the target. Assume that the observations are taken at discrete time points $T.k$, with a discretisation time step, $T$. The target state at time $k$ is expressed by

$$\mathbf{x}_k = [x_k,\ \dot{x}_k,\ \ddot{x}_k,\ y_k,\ \dot{y}_k,\ \ddot{y}_k]^T, \tag{1}$$

where $x_k$ and $y_k$ represent the position, $\dot{x}_k$ and $\dot{y}_k$ represent the velocity, and $\ddot{x}_k$ and $\ddot{y}_k$ represent the acceleration respectively. The Singer model [16], [15] yields

$$\mathbf{x}_k = \mathbf{A}(T, \alpha)\mathbf{x}_{k-1} + \mathbf{B}_u(T)\mathbf{u}_k + \mathbf{B}_u(T)\mathbf{w}_k, \tag{2}$$

where $\mathbf{u_k} = [u_{x,k},\ u_{y,k}]^T$ is the unknown discrete time command process inducing the dynamics of the system. The command process, $\mathbf{u_k}$ is modelled as a Markov chain with a finite number of states at possible levels of accelerations [16]. The matrices in (2) are given by

$$\mathbf{A}(T,\alpha) = \begin{pmatrix} \tilde{\mathbf{A}} & \mathbf{0}_{3\times3} \\ \mathbf{0}_{3\times3} & \tilde{\mathbf{A}} \end{pmatrix}, \tilde{\mathbf{A}} = \begin{pmatrix} 1 & T & T^2/2 \\ 0 & 1 & T \\ 0 & 0 & \alpha \end{pmatrix},$$

$$\mathbf{B}_u(T) = \begin{pmatrix} \tilde{\mathbf{B}}_u & \mathbf{0}_{3\times1} \\ \mathbf{0}_{3\times1} & \tilde{\mathbf{B}}_u \end{pmatrix}, \tilde{\mathbf{B}}_u = \begin{pmatrix} T^2/2 \\ T \\ 0 \end{pmatrix},$$

where $\mathbf{w}_k = [w_{x,k}, w_{y,k}]^T$ is a zero mean Gaussian distributed random variable, representing the process noise, with a covariance matrix $E[\mathbf{w}_k\mathbf{w}_k^T] = \mathbf{Q} = \sigma_w^2\mathbf{I}$. The standard deviation is denoted as $\sigma_w$ and $\alpha$ is the reciprocal of the manoeuvre time constant.

### B. Measurement Model

The RSS measurement $z_k^i$ between the $i-th$ sensor and the target at time instant $k$ is modelled as [17]

$$z_k^i = z_k^0 + 10\beta\log_{10}(d_k^i) + v_k^i, \tag{3}$$

where $z_k^0$ is the path loss at the reference distance $d^0$, ($d^0$ is normally taken as 1 m or $(d^0 \le d^i)$); $d_k^i$ is the distance between the $i-th$ sensor and the target, $\beta$ is the path loss exponent, and $v_k^i \sim \mathcal{N}(0, (\sigma_k^i)^2)$, is a zero mean Gaussian distributed random variable representing the shadowing noise. Both parameters $\beta$ and $\sigma_k^i$ are environment dependent. This model is suitable for both indoor and outdoor environments and its parameters can be configured according to different environments. To enable accurate tracking, a minimum of three distance measurements are needed. For multiple sensor measurements, the RSS between the sensors and target can be written in vector form as

$$\mathbf{z}_k = \mathbf{h}(\mathbf{x}_k) + \mathbf{v}_k, \tag{4}$$

where $\mathbf{z}_k$ represents the measurements at $n_s$ sensor nodes, i.e., $\mathbf{z}_k = (z_k^1, z_k^2, \ldots, z_k^{n_s})^T$ and $\mathbf{h}(\mathbf{x}_k) = (h(x_k^1), h(x_k^2), \ldots, h(x_k^{n_s}))^T$ is vector with entries given by the non-linear function $h_k^i = z_k^0 + 10\beta\log_{10}(d_k^i)$, for $i = 1, \ldots, n_s$, $\mathbf{z}_k \in \mathbb{R}^{n_s}$, and $n_s \ge 3$. The vector, $\mathbf{v}_k$ represents the measurements noise, with covariance matrix $E[\mathbf{v}_k\mathbf{v}_k^T] = \mathbf{C}_k$, and is assumed to be correlated in space and time.

### C. Correlated Data Model for Measurements Generation

The measurements described by (4) are assumed to have correlated noise. The correlation is both in space and time. In practice, this correlation is unknown. In the measurements, the spatial and temporal correlations are modelled as described in the following paragraph, which is based on the Gudmundson model [10]. The developed filter is used to validate the correlated measurements with the proposed shrinkage-based PF.

*1) Spatial Dependence:* The covariance between the measurements at $i-th$ and $j-th$ sensor nodes, at time instant $k$ is formulated as follows

$$C_k^{(i,j)} = \rho_k^{(i,j)}\sigma_k^{(i)}\sigma_k^{(j)}, \tag{5}$$

where $\rho_k^{(i,j)}$ is the spatial correlation given by

$$\rho_k^{(i,j)} = \exp^{(-d_k^{(i,j)}/D_c)}, \tag{6}$$

where $d_k^{(i,j)}$ is the relative distance between the two sensors and $D_c$ is the decorrelation distance [5].

*2) Temporal Dependence:* The covariance at the $i-th$ sensor, between a target measurements at time instant $k$ and $l$ is given as follows

$$C_{(k,l)}^i = \tilde{\rho}_{(k,l)}^i\tilde{\sigma}_{(k)}^i\tilde{\sigma}_{(l)}^i, \tag{7}$$

where $\tilde{\rho}_{(k,l)}^i$ is the temporal correlation given by

$$\tilde{\rho}_{(k,l)}^i = \exp^{(-d_{(k,l)}^i/D_c)}, \tag{8}$$

where $d_{(k,l)}^i$ represents the distance travelled by the target from time instant $k$ to $l$, which is given by $d_{(k,l)}^i = \sqrt{\dot{x}^2 + \dot{y}^2} \times \Delta t_{(k,l)}$; $\Delta t_{(k,l)} = t_{(l)} - t_{(k)}$.

*3) Spatio-Temporal Dependence:* Correlated measurements based on (6) and (8) up to time instant $k$ are given by

$$\mathbf{z} = [(\mathbf{z}_1^{n_s})^T, (\mathbf{z}_2^{n_s})^T, \ldots, (\mathbf{z}_k^{n_s})^T]^T, \tag{9}$$

with the covariance matrix given by

$$\mathbf{C} = \begin{bmatrix} \mathbf{C}_{1,1} & \mathbf{C}_{1,2} & \ldots & \mathbf{C}_{1,k} \\ \mathbf{C}_{2,1} & \mathbf{C}_{2,2} & \ldots & \mathbf{C}_{2,k} \\ \vdots & \vdots & \ddots & \vdots \\ \mathbf{C}_{k,1} & \mathbf{C}_{k,2} & \ldots & \mathbf{C}_{k,k} \end{bmatrix}, \tag{10}$$

where the diagonal elements of the covariance matrix captures the spatial dependence, given by

$$\mathbf{C}_{k,k} = \begin{bmatrix} (\sigma_k^{(1)})^2 & \rho_k^{(1,2)}\sigma_k^{(1)}\sigma_k^{(2)} & \cdots & \rho_k^{(1,n_s)}\sigma_k^{(1)}\sigma_k^{(n_s)} \\ \rho_k^{(2,1)}\sigma_k^{(2)}\sigma_k^{(1)} & (\sigma_k^{(2)})^2 & \cdots & \rho_k^{(2,n_s)}\sigma_k^{(2)}\sigma_k^{(n_s)} \\ \vdots & \vdots & \ddots & \vdots \\ \rho_k^{(n_s,1)}\sigma_k^{(n_s)}\sigma_k^{(1)} & \rho_k^{(n_s,2)}\sigma_k^{(n_s)}\sigma_k^{(2)} & \cdots & (\sigma_k^{(n_s)})^2 \end{bmatrix},$$

and the off-diagonal elements of the covariance matrix captures the temporal dependence, given by

$$\mathbf{C}_{k,l} = \begin{bmatrix} \tilde{\rho}^1_{(k,l)}\tilde{\sigma}^1_{(k)}\tilde{\sigma}^1_{(l)} & 0 & \cdots & 0 \\ 0 & \tilde{\rho}^2_{(k,l)}\tilde{\sigma}^2_{(k)}\tilde{\sigma}^2_{(l)} & \cdots & 0 \\ \vdots & \vdots & \ddots & \vdots \\ 0 & 0 & \cdots & \tilde{\rho}^{n_s}_{(k,l)}\tilde{\sigma}^{n_s}_{(k)}\tilde{\sigma}^{n_s}_{(l)} \end{bmatrix}.$$

The measurements at time instant $k$ are temporally correlated with the measurements at all the previous time instants. However, to limit the dimensionality of the covariance matrix, a time window retaining the measurements in the preceding time instant is used.

## III. Shrinkage Method

### A. Covariance Matrix

In practise, the covariance matrix is unknown and needs to be estimated. A simple method to estimate the covariance matrix is using the sample covariance estimator. Given a vector of RSS measurements, $\mathbf{z}_k$, at time $k$, the sample covariance matrix estimator is defined as

$$\hat{\mathbf{C}}_k = \frac{1}{P-1}\sum_{p=1}^{P}(\mathbf{z}_{kp} - \bar{\mathbf{z}}_k)(\mathbf{z}_{kp} - \bar{\mathbf{z}}_k)^T, \tag{11}$$

where $\bar{\mathbf{z}}_k$ is the sample mean and $P$ is the number of observations. The sample covariance estimate in (11) is unbiased. However, when $P < n_s$, the sample covariance matrix estimate is ill-conditioned, non-invertible, and introduces a large estimation error. This problem can be addressed by providing structure to the sample covariance matrix.

### B. Shrinkage Estimator

The shrinkage estimator combines the sample estimator with other available information in order to get better estimates of the covariance matrix. The shrinkage estimator introduced in [18] is well conditioned for small number of observations, $(P \ll n_s)$ and defined as

$$\mathbf{S} = \lambda\mathbf{T} + (1-\lambda)\hat{\mathbf{C}}, \tag{12}$$

where $\mathbf{T}$ is the target matrix and $\hat{\mathbf{C}}$ is the sample covariance matrix. The target matrix, $\mathbf{T}$ is a highly structured matrix. As a result, it has a low variance but is biased. On the other hand, $\hat{\mathbf{C}}$ has a high variance but is an unbiased estimate. The shrinkage intensity, $\lambda \in [0,1]$ captures a trade-off between the target matrix and the sample covariance matrix. There are six types of target matrix structures in [12] and each target matrix has a different variance-bias trade-off. Here, the following target matrices are used. The first target matrix is the diagonal, unit variance shrinkage target covariance given by

$$\mathbf{T}_1 = \begin{cases} 1, & \text{if } i = j \\ 0, & \text{if } i \neq j \end{cases}, \tag{13}$$

with shrinkage intensity determined by

$$\hat{\lambda}_{\mathbf{T}_1} = \frac{\sum_{i\neq j}\widehat{Var}\left(\left[\hat{\mathbf{C}}\right]_{ij}\right) + \sum_i \widehat{Var}\left(\left[\hat{\mathbf{C}}\right]_{ii}\right)}{\sum_{i\neq j}\left[\hat{\mathbf{C}}\right]_{ij}^2 + \sum_i\left(\left[\hat{\mathbf{C}}\right]_{ii} - 1\right)^2}, \tag{14}$$

where $\left[\hat{\mathbf{C}}\right]_{ij}$ refers to the elements at the $i-th$ row and $j-th$ column of the matrix $\hat{\mathbf{C}}$. The variance of the sample covariance matrix is defined as

$$\widehat{Var}\left(\left[\hat{\mathbf{C}}\right]_{ij}\right) = \frac{P}{(P-1)^3}\sum_{p=1}^{P}(v_{ijp} - \bar{v}_{ij})^2, \tag{15}$$

$$v_{ijp} = (z_{ip} - \bar{z}_i)(z_{jp} - \bar{z}_j), \tag{16}$$

$$\bar{v}_{ij} = P^{-1}\sum_{p=1}^{P} v_{ijp}, \tag{17}$$

where $\bar{z}_i$ and $\bar{z}_j$ represent the sample means, respectively. The second target matrix is the constant correlation shrinkage target covariance given by

$$\mathbf{T}_2 = \begin{cases} \left[\hat{\mathbf{C}}\right]_{ii}, & \text{if } i = j \\ \bar{\rho}\sqrt{\left[\hat{\mathbf{C}}\right]_{ii}\left[\hat{\mathbf{C}}\right]_{jj}}, & \text{if } i \neq j \end{cases}, \tag{18}$$

with shrinkage intensity determined by

$$\hat{\lambda}_{\mathbf{T}_2} = \frac{\sum_{i\neq j}\widehat{Var}\left(\left[\hat{\mathbf{C}}\right]_{ij}\right) - \bar{\rho}f_{ij}}{\sum_{i\neq j}\left(\left[\hat{\mathbf{C}}\right]_{ij} - \bar{\rho}\sqrt{\left[\hat{\mathbf{C}}\right]_{ii}\left[\hat{\mathbf{C}}\right]_{jj}}\right)^2}, \tag{19}$$

$$f_{ij} = \frac{1}{2}\left\{\sqrt{\frac{\left[\hat{\mathbf{C}}\right]_{jj}}{\left[\hat{\mathbf{C}}\right]_{ii}}}\widehat{Cov}\left(\left[\hat{\mathbf{C}}\right]_{ii}, \left[\hat{\mathbf{C}}\right]_{ij}\right) + \sqrt{\frac{\left[\hat{\mathbf{C}}\right]_{ii}}{\left[\hat{\mathbf{C}}\right]_{jj}}}\widehat{Cov}\left(\left[\hat{\mathbf{C}}\right]_{jj}, \left[\hat{\mathbf{C}}\right]_{ij}\right)\right\}. \tag{20}$$

The parameter $\bar{\rho}$ is the average correlation of all the correlations between the measurements

$$\bar{\rho} = \frac{1}{n_s(n_s-1)}\sum_{i=1}^{n_s}\sum_{j\neq 1}^{n_s}\frac{\left[\hat{\mathbf{C}}\right]_{ij}}{\left[\hat{\mathbf{C}}\right]_{ij}\left[\hat{\mathbf{C}}\right]_{ij}}. \tag{21}$$

The covariance elements are given by

$$\widehat{Cov}\Big(\Big[\hat{\mathbf{C}}\Big]_{ii}, \Big[\hat{\mathbf{C}}\Big]_{ij}\Big) =$$
$$\frac{P}{(P-1)^3}\sum_{p=1}^{P}\Big\{\Big[(z_{ip}-\bar{z}_i)^2-\bar{v}_{ii}\Big]\Big[(z_{ip}-\bar{z}_i)(z_{jp}-\bar{z}_j)-\bar{v}_{ij}\Big]\Big\}, \tag{22}$$

and similarly

$$\widehat{Cov}\Big(\Big[\hat{\mathbf{C}}\Big]_{jj}, \Big[\hat{\mathbf{C}}\Big]_{ij}\Big) =$$
$$\frac{P}{(P-1)^3}\sum_{p=1}^{P}\Big\{\Big[(z_{jp}-\bar{z}_j)^2-\bar{v}_{jj}\Big]\Big[(z_{ip}-\bar{z}_i)(z_{jp}-\bar{z}_j)-\bar{v}_{ij}\Big]\Big\}. \tag{23}$$

In most cases, $\hat{\lambda} \in [0,1]$. However, in cases where $\hat{\lambda} \notin [0,1]$, the following bound is imposed:

$$\hat{\lambda} = \max(0, \min(1, \hat{\lambda})).$$

## IV. Particle Filtering with Shrinkage for Dealing with Correlated Measurements

Particle filtering, also known as sequential Monte Carlo method is one of the powerful methods that can be used for tracking applications. The target motion model in (1)-(2) and the observation model in (3)-(4) can be written in the following general form:

$$\mathbf{x}_k = f(\mathbf{x}_{k-1}, \mathbf{w}_k), \tag{24}$$
$$\mathbf{z}_k = h(\mathbf{x}_k, \mathbf{v}_k), \tag{25}$$

where $\mathbf{w}_k$ and $\mathbf{v}_k$ are independent noise processes with known probability distribution function. Functions $f(\cdot)$ and $h(\cdot)$ are non-linear in general. In this section, (24) and (25) constitute the whole model for the target mobility and correlated sensor measurements. In PF tracking, the target state, $\mathbf{x}_k$ has to be estimated recursively based on the received sensor measurements $\mathbf{z}_k = \{z_k^1, z_k^2, \ldots, z_k^{n_s}\}, \mathbf{x}_k \in \mathbb{R}^{n_s}$. From a Bayesian point of view, this implies obtaining estimates of the state posterior density function, that is

$$p(\mathbf{x}_k|\mathbf{z}_k) = \frac{p(\mathbf{z}_k|\mathbf{x}_k) \times p(\mathbf{x}_k|\mathbf{z}_{k-1})}{p(\mathbf{z}_k|\mathbf{z}_{k-1})}, \tag{26}$$

where $p(\mathbf{z}_k|\mathbf{x}_k)$ is the likelihood function, $p(\mathbf{x}_k|\mathbf{z}_{k-1})$ is the state prior density function, and $p(\mathbf{z}_k|\mathbf{z}_{k-1})$ is the normalizing constant. By using a set of particles $\mathbf{x}_k^{(i)}, i = 1, \ldots, N_p$, where $N_p$ is the total particles, and their corresponding weights $W_k^{(i)}$, the state posterior density function can be further described as follows

$$p(\mathbf{x}_k|\mathbf{z}_k) = \sum_{i=1}^{N_p} \hat{W}_k^{(i)} \times \mathbf{x}_k^{(i)}, \tag{27}$$

where the weights are normalized such that $\sum_i \hat{W}_k^{(i)} = 1$. The estimated position of the target is obtained by the weighted sum of particles. In general, the PF works based on three important stages which are the prediction stage, measurement stage and resampling stage. During the prediction stage, each particle transition state is generated according to the target mobility model. In the measurement stage, each particle's weight is re-evaluated based on the likelihood function. Finally, in the resampling stage, those particles with small weights are eliminated and larger weights are replicated. The residual resampling algorithm [19], [8] is applied in this paper.

### A. Likelihood Function of Particle Filter

The likelihood function is used to re-evaluated the weight of the particle which is given by

$$\mathcal{L}(\mathbf{z}_k|\mathbf{x}_k) = \{(2\pi)^{n_s}|\mathbf{C}_k|\}^{-\frac{1}{2}}\ \exp^{\{-0.5(\mathbf{z}-\hat{\mathbf{z}})^T\mathbf{C}_k^{-1}(\mathbf{z}-\hat{\mathbf{z}})\}}, \tag{28}$$

where the parameters, $\mathbf{z}$ and $\hat{\mathbf{z}}$ represent the actual and predicted RSS measurements, $\mathbf{C}_k$ is the measurement noise covariance matrix at time $k$, and $n_s$ is the number of sensors, and $|\cdot|$ denotes the matrix determinant. In this paper, the shrinkage estimator in (12) is introduced to estimate the covariance matrix in (28) to improve the tracking performance of the PF.

### B. A Particle Filter with Shrinkage

The developed PF combined with the shrinkage method is based on the models proposed in [16]. The following algorithm describes the proposed method.

I. For $k = 0$, and $i = 1, \ldots, N_p$

***(1) Initialization***

Draw $N_p$ particles $\mathbf{x}_0^{(i)}$ from the prior distribution $p(\mathbf{x}_0)$ and set the initial weights $W_0^{(i)} = 1/N_p$.

II. For $k = 1, 2, \ldots,$ and $i = 1, \ldots, N_p$

***(2) Prediction Step***

Predict the new particles using (2)
$\mathbf{x}_k^{(i)} = \mathbf{A}(T,\alpha)\mathbf{x}_{k-1}^{(i)} + \mathbf{B}_u(T)\mathbf{u}_k^{(i)} + \mathbf{B}_u(T)\mathbf{w}_k^{(i)}$,
with noise realisations $\mathbf{w}_k^{(i)} \sim \mathcal{N}(\mathbf{0}, \mathbf{Q})$.

***(3a) Shrinkage Covariance Estimator***

Estimate the covariance matrix using the shrinkage estimator given by $\mathbf{S} = \lambda\mathbf{T} + (1-\lambda)\hat{\mathbf{C}}$.
This estimator is explicitly defined in $(12) - (23)$.

***(3b) Measurement Update***

Compute the weights of the received measurements using $W_k^{(i)} = W_{k-1}^{(i)} \times \mathcal{L}(\mathbf{x}_k|\mathbf{z}_k)$, where $\mathcal{L}(\mathbf{x}_k|\mathbf{z}_k)$ is given in (28) where the estimated covariance matrix $\mathbf{C} = \hat{\mathbf{S}}$ is used. After that, normalize the weights using $\hat{W}_k^{(i)} = W_k^{(i)} / \sum_{i=1}^{N_p} W_k^{(i)}$.

***(4) Output Estimate***

The posterior mean $E[\mathbf{x}_k|\mathbf{z}_k]$, is defined as
$\hat{\mathbf{x}}_k = E[\mathbf{x}_k|\mathbf{z}_k] = \sum_{i=1}^{N_p} \hat{W}_k^{(i)} \times \mathbf{x}_k^{(i)}$.

***(5) Resampling Step***

The residual resampling algorithm [19], [8], [20] is applied.
Set $k \to k+1$ and return to step 2.

## V. Performance Evaluation

The shrinkage-based PF, with a target matrix $\mathbf{T}_1$ in (13) and $\mathbf{T}_2$ in (18) is used to track the movement of a single target. The performance of the PF is compared with and without the shrinkage. The sensor nodes $(n_s = 9)$ are uniformly deployed and form a square grid. In order to maintain full coverage and reduce the tracking error, all sensors move in the direction towards the target but do not cross their designated grid. The speed of the mobile sensors varies within a specified range. A time window, $\Delta t = 1$ is used to capture the temporal correlation of the measurements at the sensor nodes. The other parameters are given in Table I.

TABLE I: Simulation Parameters for Target Tracking

| | |
|---|---|
| Number of sensor (anchor) nodes $n_s$ | 9 |
| Speed of sensor node | $(0.05 - 0.15)$ $ms^{-1}$ |
| Number of target node | 1 |
| Minimum speed of target node $V_{min}$ | 0.05 $ms^{-1}$ |
| Maximum speed of target node $V_{max}$ | 5.04 $ms^{-1}$ |
| Reciprocal manoeuvre time constant $\alpha$ | 0.5 |
| Discretisation time step $T$ | 1.0 $s$ |
| Number of Particles $N_p$ | 500 |
| Standard deviations $\sigma_k^i, \sigma_k^j$ in (5) | $[0 - 4]$ dB |
| Standard deviations $\hat{\sigma}_k^i, \hat{\sigma}_l^i$ in (7) | $[0 - 4]$ dB |
| Path loss index $\beta$ | 3 |
| Decorrelation distance $D_c$ | 40 m |
| Time window for temporal correlation $\Delta t$ | 1 |
| Command Processes $\mathbf{u}_k$ | $\{[1.0\ 0.0]^T, [0.0\ 1.0]^T\}$ |

The performance validation is carried out using a PC computer with an Intel core 3.3 GHz processor, 4 GB RAM, and 465 GB hardrive. The proposed algorithm is repeatedly executed with a single execution would take 1.37 seconds to complete. Figure 1 compares the performance of the PF method when the shrinkage covariance matrix estimate is applied ($\mathbf{C} = \mathbf{S}$) and when no covariance matrix is used ($\mathbf{C} = \mathbf{I}$). In the measurement stage of the PF method, the likelihood is calculated using (28). The tracking accuracy of the methods is evaluated using root mean square error (RMSE). This measure is used to assess the difference between the true and the estimated position of the target. In the simulation, the shrinkage-based PF performs considerably better than PF without shrinkage for all number of observations. The accuracy of the target tracking increases when a large number of observations is available. The shrinkage-based PF with the target matrix $\mathbf{T}_1$ achieves lower RMSE value compared to that with target matrix $\mathbf{T}_2$ when dealing with a limited number of observations. When target matrix $\mathbf{T}_1$ is used in (12), the estimated covariance matrix, $\hat{\mathbf{S}}$ is calculated by an equally weighted terms. However, when target matrix $\mathbf{T}_2$ is used, then the estimated covariance matrix, $\hat{\mathbf{S}}$ is closer to the first term in (12). For a larger number of observations, $(P > 8)$ there is no obvious difference in the position RMSE between the two target matrices.

In Figure 2, the tracking accuracy is compared for different values of shadowing variance in the path-loss measurements. When the value of the noise variance is increased, the position RMSE value also increases for all the methods. However, the shrinkage-based PF still outperforms the PF without shrinkage.

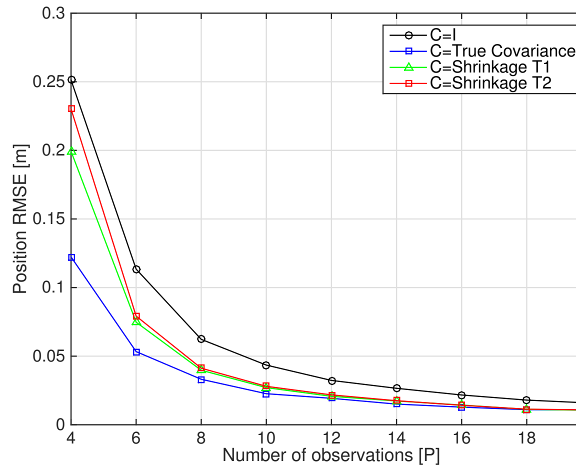


Fig. 1: Performance comparison between PF tracking with and without shrinkage covariance matrix estimation.

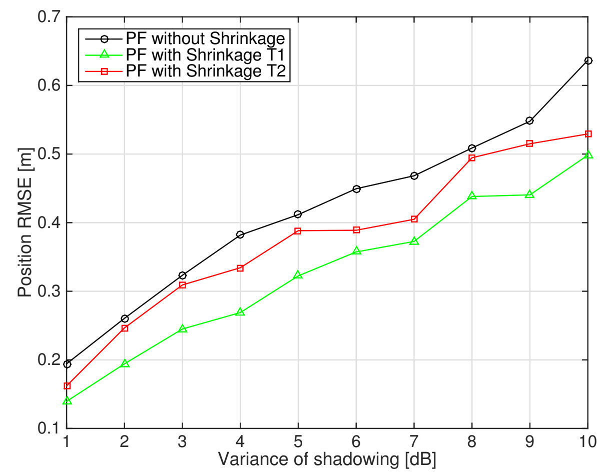


Fig. 2: Position error (RMSE) comparison over different number of selected sensor nodes (anchors).

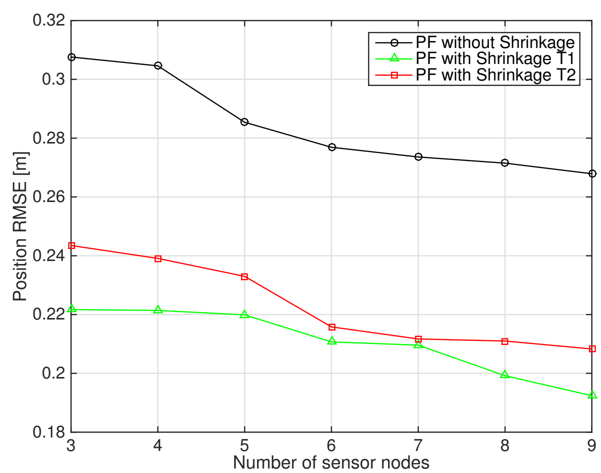


Fig. 3: Position error (RMSE) comparison over different number of selected sensor nodes (anchors).

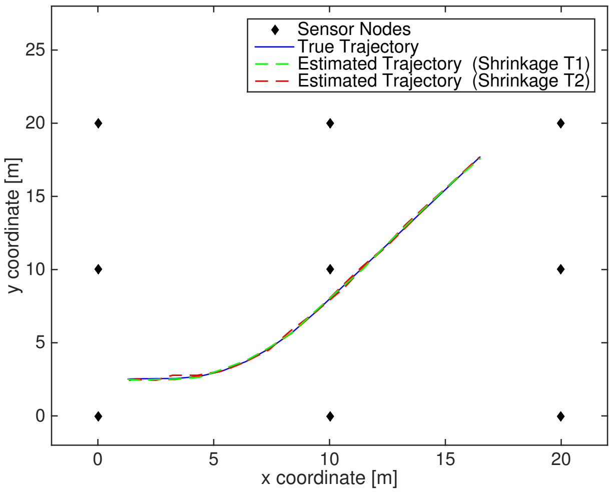


Fig. 4: Sensor deployment and trajectory of moving target

The shrinkage-based PF with the target matrix $\mathbf{T}_1$, has lower tracking error compare to shrinkage estimator with the target matrix $\mathbf{T}_2$.

Figure 3 shows the value of the position error (RMSE) against the number of sensor nodes. The result confirms that when a larger number of sensor nodes is used to perform tracking, position estimation is improved due to the availability of more data in the estimation process. The shrinkage-based PF with the target matrix $\mathbf{T}_1$ has a slightly smaller position error (RMSE) compared to the case with target matrix $\mathbf{T}_2$. Overall, the shrinkage-based PF has significantly better results compared to the PF without the shrinkage estimator. Figure 4 shows the sensor nodes deployment, true target trajectory and estimated target trajectory using the shrinkage-based PF with the target matrices $\mathbf{T}_1$ and $\mathbf{T}_2$.

## VI. Conclusions

Target tracking in WSNs with correlated spatial and temporal measurement noise is studied. A shrinkage-based PF algorithm for a single target tracking is proposed. The shrinkage estimate is used in the PF to calculate the likelihood function. Finally, a performance evaluation of the shrinkage-based PF is carried out through simulations. The results show that the shrinkage-based PF outperforms the PF without the shrinkage for a single target tracking.

## Acknowledgements

A. Kiring acknowledges the support from the Ministry of Education Malaysia via Skim Latihan Akademik IPTA (SLAI), L. Mihaylova and N. Salman acknowledge the support from the UK Engineering and Physical Sciences Research Council (EPSRC) for the support via the Bayesian Tracking and Reasoning over Time (BTaRoT) grant EP/K021516/1.

## References

[1] R. Peng and M. Sichitiu, "Angle of arrival localization for wireless sensor networks," in *IEEE Sensor and Ad Hoc Commun. and Networks*, vol. 1, pp. 374–382, Sept 2006.

[2] R. Li, Y. Li, Y. Shen, L. Liu, and Q. Cao, "An optimization algorithm for wireless sensor networks localization using multiplier method," in *3rd International Joint Conf. on Computational Science and Optimization*, vol. 2, pp. 337–341, May 2010.

[3] J. Xiao, L. Ren, and J. Tan, "Research of tdoa based self-localization approach in wireless sensor network," in *IEEE/RSJ International Conf. on Intelligent Robots and Systems*, pp. 2035–2040, Oct 2006.

[4] S. Tomic, M. Beko, R. Dinis, and M. Raspopovic, "Distributed rss-based localization in wireless sensor networks using convex relaxation," in *International Conf. on Computing, Networking and Communications*, pp. 853–857, Feb 2014.

[5] N. Salman, L. Mihaylova, and A. Kemp, "Localization of multiple nodes based on correlated measurements and shrinkage estimation," in *Sensor Data Fusion: Trends, Solutions, Applications*, pp. 1–6, Oct 2014.

[6] Z. Zaidi and B. Mark, "A mobility tracking model for wireless ad hoc networks," in *IEEE International Conf. on Wireless Commun. and Networking*, vol. 3, pp. 1790–1795, March 2003.

[7] Z. Zaidi and B. Mark, "Mobility estimation for wireless networks based on an autoregressive model," in *IEEE Global Telecommunications Conf.*, vol. 6, pp. 3405–3409, Nov 2004.

[8] E. Wan and R. Van Der Merwe, "The unscented kalman filter for nonlinear estimation," in *IEEE Adaptive Systems for Signal Processing, Commun., and Control Symposium*, pp. 153–158, 2000.

[9] D. Simon, *Optimal State Estimation: Kalman, H Infinity, and Nonlinear Approaches*. Wiley-Interscience, 2006.

[10] M. Gudmundson, "Correlation model for shadow fading in mobile radio systems," *Electronics Letters*, vol. 27, pp. 2145–2146, Nov 1991.

[11] O. Ledoit and M. N. Wolf, "Honey, I Shrunk the Sample Covariance Matrix," *SSRN Electronic Journal*, 2003.

[12] J. Schäfer and K. Strimmer, "A shrinkage approach to large-scale covariance matrix estimation and implications for functional genomics," *Statistical Applications in Genetics and Molecular Biology*, vol. 4, 2005.

[13] B. Mark and Z. Zaidi, "Robust mobility tracking for cellular networks," in *IEEE International Conf. on Commun.*, vol. 1, pp. 445–449, 2002.

[14] Z. Zaidi and B. Mark, "Real-time mobility tracking algorithms for cellular networks based on kalman filtering," *IEEE Transactions on Mobile Computing*, vol. 4, pp. 195–208, March 2005.

[15] Z. Yang and X. Wang, "Joint mobility tracking and hard handoff in cellular networks via sequential monte carlo filtering," in *Proc. IEEE Joint Conf. of the Computer and Commun. Socities*, vol. 2, pp. 968–975, 2002.

[16] L. Mihaylova, D. Angelova, S. Honary, D. Bull, C. Canagarajah, and B. Ristic, "Mobility tracking in cellular networks using particle filtering," *IEEE Transactions on Wireless Communications*, vol. 6, pp. 3589–3599, October 2007.

[17] K. Pahlavan and A. H. Levesque, *Wireless Information Networks (Wiley Series in Telecommunications and Signal Processing)*. John Wiley & Sons, 2005.

[18] O. Ledoit and M. N. Wolf, "A well-conditioned estimator for large-dimensional covariance matrices," *Journal of Multivariate Analysis*, vol. 88, no. 2, pp. 365 – 411, 2004.

[19] J. S. Liu and R. Chen, "Sequential monte carlo methods for dynamic systems," *Journal of the American Statistical Association*, vol. 93, pp. 1032–1044, 1998.

[20] R. Douc and O. Cappe, "Comparison of resampling schemes for particle filtering," in *Proc. of the 4th International Symposium on Image and Signal Processing and Analysis*, pp. 64–69, Sept 2005.